21th International Conference on Composite Materials
Xi'an, 20-25th August 2017

THICK-LEVEL-SET MODELING OF THE DYNAMIC DOUBLE CANTILEVER BEAM TEST

Y. Liu, F.P. van der Meer, L.J. Sluys

Faculty of Civil Engineering and Geosciences, Delft University of Technology
PO Box 5048, 2600 GA Delft, The Netherlands
Email: y.liu-7@tudelft.nl

Keywords: Thick level set, Dynamic fracture, Double cantilever beam, Crack arrest

ABSTRACT

In this paper, the thick-level-set method is used to model stable and unstable (stick/slip) crack propagation in the dynamic double cantilever beam (DCB) test for unidirectional composite laminates. The thick-level-set method uses a predefined damage profile to describe the fracture process zone and allows for accurate evaluation of the global energy release rate. A phenomenological model is introduced to calculate the crack speed as a function of the energy release rate. The potential capability of the proposed approach is demonstrated by simulating a series of dynamic DCB tests under variable test rates.

1 INTRODUCTION

Delamination is one of the major damage mechanisms for composite laminates under dynamic loading. It is believed that the interlaminar fracture toughness depends on the loading rate [1]. This, with regard to numerical modeling, motivates the development of rate-dependent cohesive zone models (CZM). In terms of experimental characterization, the dynamic double cantilever beam (DCB) test is used to measure the dynamic fracture toughness. In a comparison between numerical results obtained with a rate-dependent CZM and experimental measurements, a good agreement can only be found when crack arrest and re-initiation phenomena from the experiments are ignored. Inability of the CZM approach to reproduce these phenomena from this basic test limits the suitability of this approach for predictive simulations in more complex cases.

In this contribution, the thick-level-set (TLS) model [2, 3] is used to simulate the dynamic DCB test, including repeated crack arrest and re-initiation. The TLS model was first introduced by Möes et al. [2] for the modeling of damage growth in a continuum damage framework. Contrary to conventional continuum damage mechanics, the damage in the TLS is not a direct function of the local strain but rather a function of the distance to a moving damage front. The movement of the damage front is achieved by evaluating the configurational force across the damage band. The TLS model was translated to interface elements by Latifi et al. [3] to provide an alternative to the CZM for interfacial cracking. An advantage of the TLS for dynamics is that a relationship between the energy release rate and crack speed can be used as input of the model.

Ravi-Chandar [4] introduced a dynamic fracture criterion in which the three states of a crack, i.e. initiation, propagation and arrest, are explicitly differentiated. The dynamic stress intensity factor K, as a measurement of the dynamic stress field near the crack tip, is used as an indicator of the state in which the crack should be under a given loading condition. Inspired by the above criterion, a new phenomenological model on the relation between energy release rate and crack speed is introduced. Both stable and unstable (stick/slip) crack propagation observed in the dynamic DCB test can be simulated with the presented TLS approach.

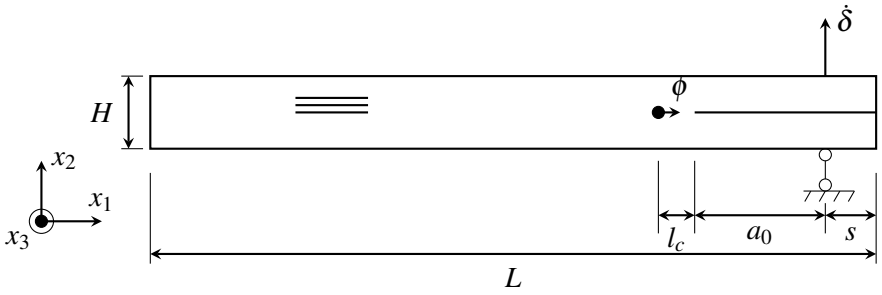

Figure 1: Double cantilever beam

2 METHOD

The dynamic double cantilever beam test of an unidirectional composite laminate under a series of constant loading rates $\dot{\delta}$ is simulated by implicit dynamic numerical analysis (see Fig. 1). The constant velocity $\dot{\delta}$ is applied at the top surface of the arm and the vertical degree-of-freedom of the node symmetric to the loading point with the crack plane is constrained. The bulk material of the beam is represented by plane strain triangular elements with an orthotropic linear elastic constitutive model. The middle surface between the two arms is modeled with interface elements, in which damage is described with the TLS approach. A damage band of length l_c is predefined ahead of the initial crack tip. The signed distance from the front of the damaged band is defined as the level set field ϕ. Damage d is related to the level set field ϕ by:

$$d(\phi) = \begin{cases} 0, & \phi < 0 \\ \text{atan}\left(c_1 \frac{\phi}{l_c}\right) \cdot \text{atan}(c_1)^{-1}, & 0 < \phi < l_c \\ 1, & \phi > l_c \end{cases}$$

where atan$(\cdot)$ is an arc-tangent function and c_1 determines the shape of the damage distribution. The possible contact among the upper surface and lower surface of the initial crack is considered by interface elements with penalty stiffness. At the end of each load step, the energy release rate G is calculated. Then the crack speed V is determined by a new phenomenological model and finally the level set field is updated according to the calculated crack speed.

As key assumption in the model, a function between energy release rate G and crack speed V is explicitly introduced (see Fig. 2). This function is inspired by the relation between K and V proposed by Ravi-Chandar [4]. The crack starts to grow when the energy release rate G reaches the crack initiation toughness G_i. Crack growth starts at a nonzero crack speed $V(G_i)$. During crack growth, the crack speed V is related to the energy release rate G according to an exponential function which possesses three features: (1) the crack speed has a maximum value V_m ; (2) the $V(G)$ curve has a positive slope, representing the influence of increased microcracking on the fracture toughness; (3) the crack speed jumps from a finite value to zero when the energy release rate drops below the crack arrest toughness G_a.

The function between crack speed V and energy release rate G during the propagation phase is:

$$V = V_m(1 - e^{-\alpha G}) \tag{1}$$

in which V_m is the maximum crack speed and α is a coefficient that can be determined by:

$$\alpha = -\frac{1}{G_a} \ln\left(1 - \frac{V_a}{V_m}\right) \tag{2}$$

where V_a is the crack speed at which arrest occurs and G_a is the arrest toughness of the material.

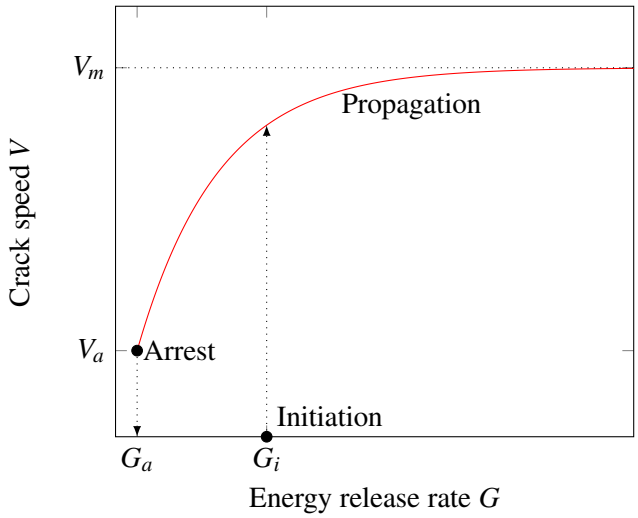

Figure 2: Relation between crack velocity V and energy release rate G

3 RESULTS

The dynamic DCB test is simulated for a series of constant test rates, namely 0.01, 1.0, 6.5 and 10.0 m/s. The dimensions adopted for each test are the same, i.e. $L = 200.0$ mm, $H = 3.0$ mm, $a_0 = 35.0$ mm, $s = 7.1$ mm (Fig. 1). The x_1-axis of an orthonormal coordinate system is set to be aligned with fibre direction and the x_3-axis is perpendicular to the crack plane. The material parameters of the bulk material are: density $\rho = 1540$ kg/m^3, Young's modulus $E_1 = 130.0$ GPa, $E_2 = 8.0$ GPa, shear modulus $G_{12} = 5.0$ GPa, and Poisson ratio $\nu_{12} = 0.28$, $\nu_{23} = 0.43$. The value of parameters used in Equation (1) are: $l_c = 0.9$ mm and $c_1 = 15$. The values for G_i, G_a, V_m and V_a are 1.5 N/mm, 0.5 N/mm, 500 m/s and 5 m/s, respectively.

The numerical simulation results are displayed in Fig. 3-7. Fig. 3 shows the evolution of crack length L, crack speed V and energy release rate G with time for the test rate of 0.01 m/s. The curve representing the crack length displays an unstable (stick/slip) type with multiple crack arrests. This unstable type of crack growth conforms with the variation of energy release rate with time (see Fig. 3c). At early loading stage when the crack is not initiated, the energy release rate G is a parabolic function of time. This is in line with the theoretical solution by using the modified beam theory [5]. As soon as G reaches the initiation toughness G_i (marked by the upper dotted line), the crack is initiated with a speed of 14.85 m/s as it is defined by the proposed phenomenological model. At the same time the energy release rate G drops immediately.

There exist two competing mechanisms dominating the evolution of the energy release rate G. The one that causes G to increase is the remote loading and its contribution is determined by the applied loading rate. The other one that causes G to decrease is crack growth and its influence is determined by the crack speed. Since the current loading rate, i.e. 0.01 m/s, is relatively small, the gain of energy release rate by the remote loading can not compensate for the loss of energy release rate by the crack growth. This is why the energy release rate keeps decreasing after crack initiation. When the energy release rate G drops to the arrest toughness G_a (indicated by the lower dotted line), the crack is arrested and the crack speed becomes zero instantly. Afterwards, the continuous loading on the beam causes the energy release rate G to increase again until the initiation toughness G_i is reached again and the arrested crack is re-initiated. What follows is that the crack experiences "initiation-propagation-arrest" cycles during the test. It is observed that the needed time for an arrested crack to re-initiate is longer for later "initiation-propagation-arrest" cycles. This observation is also in agreement with the modified beam theory, which states that under quasi-static loading conditions with given loading rate the time it takes for G to grow from G_a to G_i increases with increasing crack length.

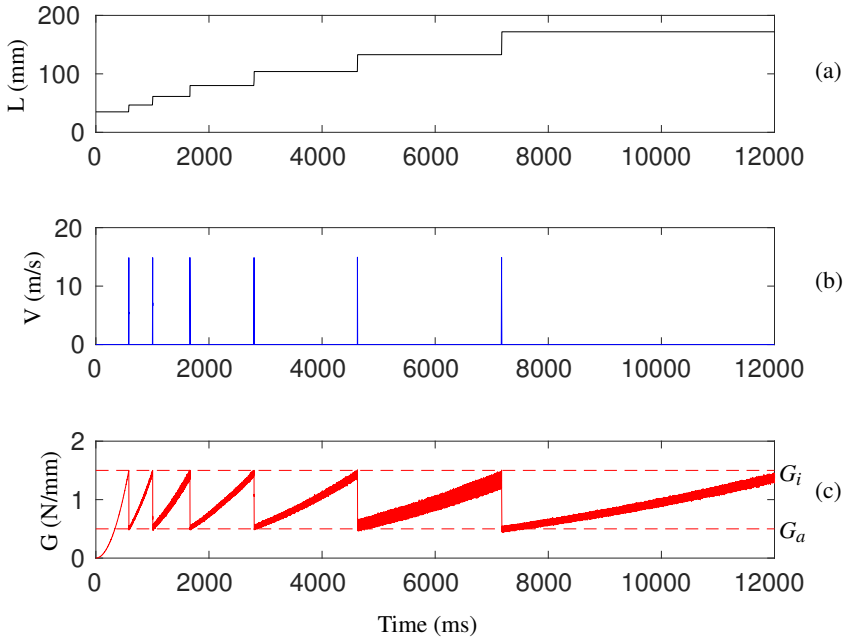

Figure 3: Time evolution of (a) crack length L; (b) crack speed V; (c) energy release rate G for the test rate of 0.01 m/s

For a higher test rate of 1.0 m/s, the development of crack length L, crack speed V and energy release rate G during the test are plotted in Fig. 4. Similar to the previous test case, the crack growth exhibits an unstable (stick/slip) type. In Fig. 4a, it can be observed that there are 5 plateaus during which time periods the crack does not grow and the crack speed is zero (see Fig. 4b). Initially, the energy release rate increases in a parabolic manner. This is consistent with the modified beam theory [5], which means that under the current test rate the theory is still an appropriate approximation for calculating the energy release rate before the crack is initiated.

However, there are a few differences observed in the current test compared with the previous test case. Most notably, the number of crack arrest events is smaller than the previous case which means that the crack is less easily arrested. This is because the decrease of the energy release rate caused by crack growth is canceled to a larger extent by the remote loading of the larger test rate case.

Fig. 5 shows the variation of crack length L, crack speed V and energy release rate G at the test rate of 6.5 m/s. The crack grows in a continuous manner and crack arrest does not occur (Fig. 5a and 5b). This continuous crack growth pattern can be understood by inspecting the variation of energy release rate shown in 5c. At the early loading phase, the energy release rate G also grows in a parabolic manner until it reaches the initiation toughness G_i. After that, G experiences an oscillatory increasing branch until it reaches a maximum value around 1.74 N/mm, followed by a gradually decreasing branch.

The reason for G to increase is that the test rate is relatively large so the increase of G by the remote loading is large enough to compensate the loss of energy release rate due to crack propagation. However, as the length of the crack becomes larger the influence of crack growth becomes more dominant, which could be understood by examining the equation to compute the energy release rate in the modified beam theory [5].

This phenomenon is more pronounced for the even larger test rate of 10.0 m/s (see Fig. 6), where there is no crack arrest present during the test either. Similarly, after the energy release rate reaches the initiation toughness, it keeps increasing until reaching a maximum value around 2.13 N/mm (see Fig. 6c) followed by a decreasing branch. The maximum energy release achieved in the current case is larger than the maximum value obtained for the smaller test rate case of 6.5 m/s. This is because the crack initiates at the same speed, 14.85 m/s, in both cases while the loading rate is larger for the test rate of 10.0 m/s case. There exist some other differences between the two cases. For instance, the increase of

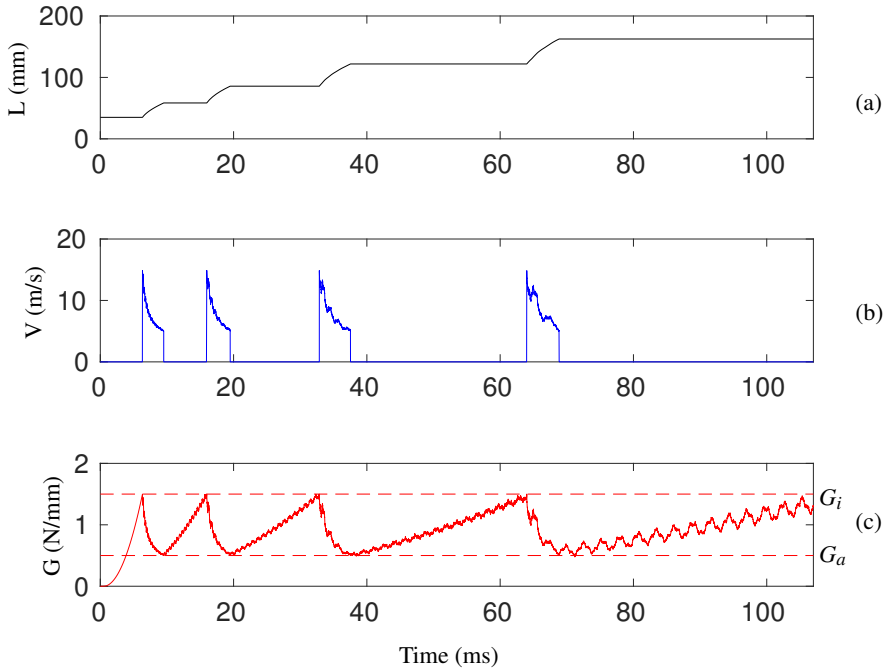

Figure 4: Time evolution of (a) crack length L; (b) crack speed V; (c) energy release rate G for the test rate of 1.0 m/s

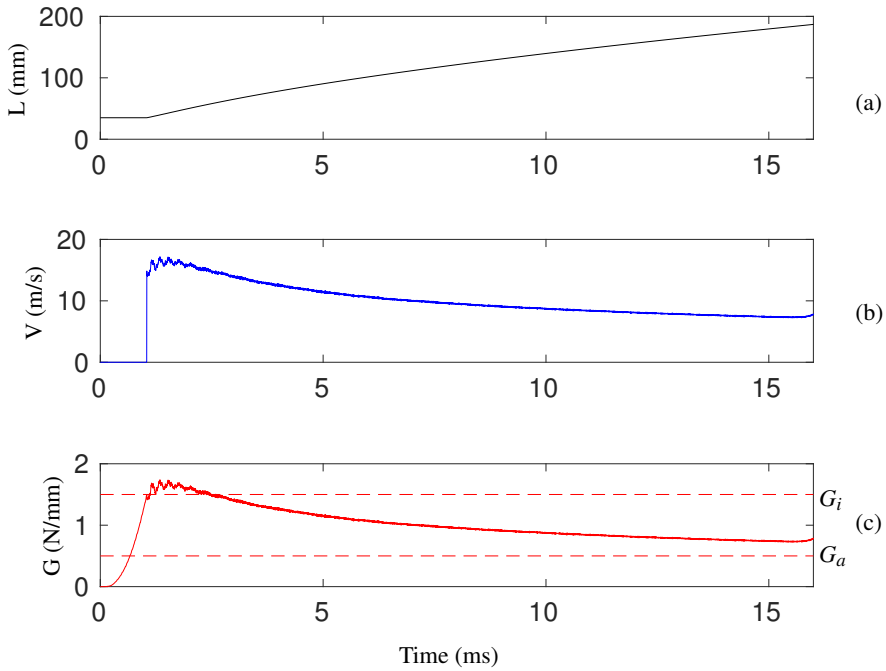

Figure 5: Time evolution of (a) crack length L; (b) crack speed V; (c) energy release rate G for the test rate of 6.5 m/s

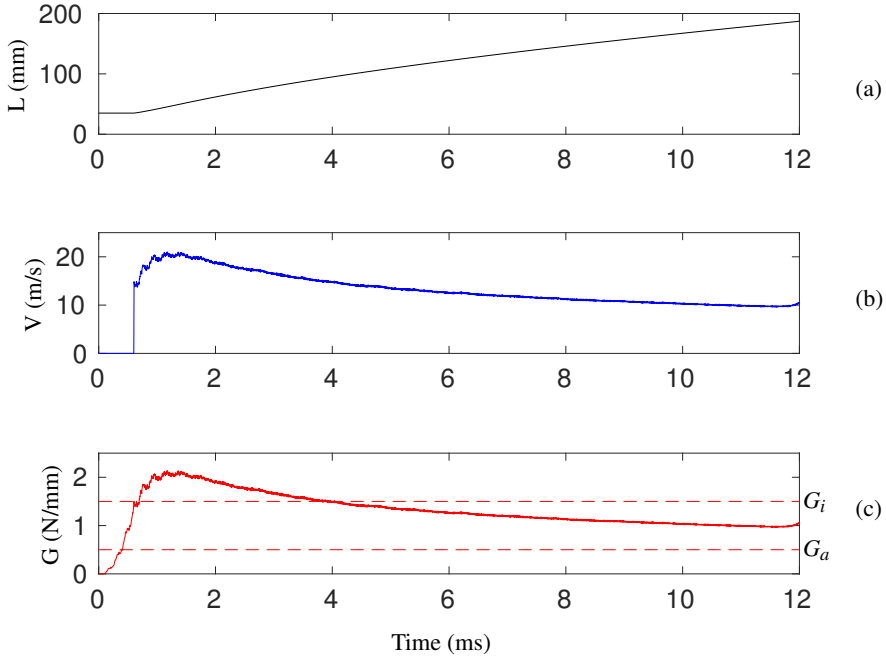

Figure 6: Time evolution of (a) crack length L; (b) crack speed V; (c) energy release rate G for the test rate of 10.0 m/s

energy release rate before the first initiation event shows significant oscillations (see Fig. 6c). This is due to the fact that more high frequency components are activated under a higher test rate and thus the assumptions made in the modified beam theory become less reasonable.

The force-displacement curve predicted by the current numerical model shows two different types for the unstable and stable propagation scenarios. The force-displacement curve for test rate of 1.0 m/s, as an example of unstable crack propagation, is plotted in Fig. 7a. The force-displacement curve for a test rate of 10.0 m/s is plotted in Fig. 7b as an example of stable crack propagation. It is seen from Fig. 7a that the force-displacement curve for an unstable crack propagation possesses a saw-teeth shape. This can be understood in the following manner. The initial linear increasing part in the force-displacement curve corresponds to the time period when the crack is not initiated and the material in the beam is still in elastic state. After the crack initiates, the force gradually decreases until the crack is arrested (Fig. 7a). After the crack is arrested, the force builds up again. After the crack is re-initiated, the force then decreases. This type of force-displacement curve is also observed in experiments [1]. For stable crack propagation seen in the test rate of 10.0 m/s, the force-displacement does not show this saw-teeth pattern. Visible oscillations are mainly due to the dynamic response of the structure.

4 CONCLUSIONS

The proposed numerical model uses the TLS concept to implement a phenomenological relation between crack speed V and energy release rate G. This study shows the potential ability of this new numerical framework to simulate the dynamic DCB test. By investigating a series of tests under different loading rates, it is concluded that the features predicted by the proposed numerical model are: (1) a transition from unstable to stable crack propagation for increasing test rates is observed; (2) unstable crack propagation leads to a saw-teeth shaped force-displacement curve while stable crack propagation results in a force-displacement curve resembling a quasi-static curve except for a certain amount of oscillations; (3) the average crack velocity increases as the test rate increases. Possible influence of strain rate-dependency, thermomechanical effect and geometry dependency on the $V(G)$ relation will be subject to future research.

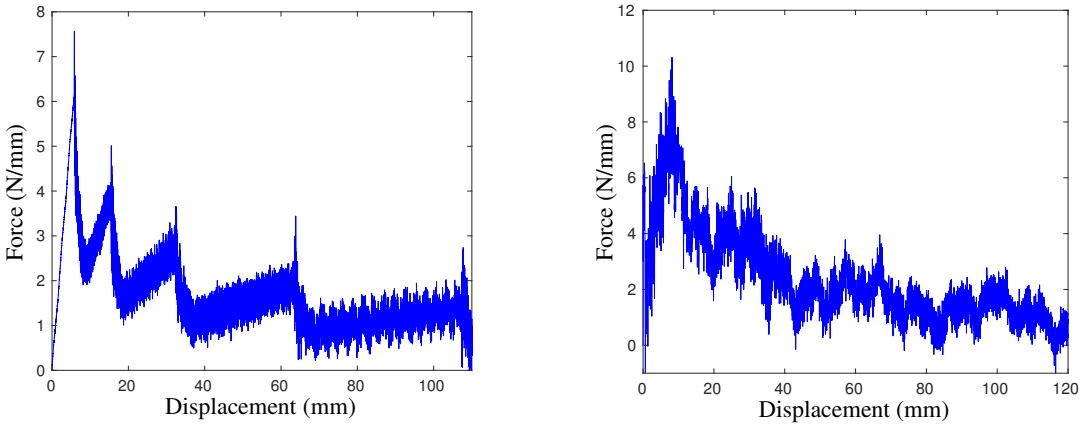

Figure 7: Force-displacement curve of test rate of (a) 1.0 m/s; (b) 10.0 m/s

REFERENCES

[1] B.R.K. Blackman, J. P. Dear, A.J. Kinloch, H. Macgillivray, Y. Wang, J. G. Williams and P. Yayla, The failure of fibre composites and adhesively bonded fibre composites under high rates of test. *Journal of Materials Science*, **30(23)**, 1995, pp. 5885-5900 (doi: 10.1007/BF01151502).

[2] N. Möes, C. Stolz, P.E. Bernard and N. Chevaugeon, A level set based model for damage growth: the thick level set approach. *International Journal for Numerical Methods in Engineering*, **86(3)**, 2011, pp. 358-380 (doi: 10.1002/nme.3069).

[3] M. Latifi, F.P. van der Meer and L.J. Sluys, An interface thick level set model for simulating delamination in composites, *International Journal for Numerical Methods in Engineering*, 2016 (doi: 10.1002/nme.5463).

[4] K. Ravi-Chandar, *Dynamic fracture*, Elsevier, 2004.

[5] B.R.K. Blackman, A.J. Kinloch, Y. Wang and J.G. Williams, The failure of fibre composites and adhesively bonded fibre composites under high rates of test, *Journal of Materials Science*, **31(17)**, 1996, pp. 4451-4466 (doi: 10.1007/BF00366341).